# NMR and ab Initio Studies of Amination of Ketenimine: Direct Evidence for a Mechanism Involving a Vinylidenediamine as an Intermediate

Kuangsen Sung,* Shu-Hwa Wu, Ru-Rong Wu, and Shu-Yi Sun

*Department of Chemistry, National Cheng Kung University, Tainan, Taiwan, ROC*

*kssung@mail.ncku.edu.tw*

*Received January 15, 2002*

High-level ab initio calculations were carried out in both gas phase and solvent ($\epsilon = 35.9$) to estabilish that the amination of ketenimine proceeds via amine addition across the C═N bond rather than the C═C bond, followed by tautomerization to form amidine product. The HOMO of ketenimine is perpendicular to its molecular plane with the largest coefficient on $C_\beta$, while the LUMO is in its molecular plane with the largest coefficient on $C_\alpha$. Amination of ketenimine involves in-plane attack of amine nucleophile on $C_\alpha$ (LUMO) of ketenimine. The labile vinylidenediamine intermediate *trans*-**11** for the reaction of ketenimine **10** with *n*-butylamine was directly observed by means of low-temperature proton NMR spectra. The evidence confirms that the amination reaction is stepwise and proceeds via *n*-butylamine addition across the C═N bond of ketenimine **10** rather than the C═C bond, followed by a slower tautomerization of vinylidenediamine *trans*-**11** to amidine **12**. Even though the second step is much slower, the first step involving amine addition across the C═N bond is kinetic control. Surprisingly, in the reaction of **10** with *n*-$BuNH_2$, attack of *n*-$BuNH_2$ syn to the phenyl group on $C_\beta$ of **10** is preferred, even though this produces a less stable product (*trans*-**11**); attack of *n*-$BuNH_2$ anti to phenyl group on $C_\beta$ of **10** is lacking and results in serious nonbonding interactions between the two phenyls of the ketenimine, as they are pushed together in this transition state.

## Introduction

Ketenimines were first prepared by Staudinger and Hauser in the 1920s,[1] and the chemistry has been reviewed.[2c−e] The ketenimines are isoelectronic with allenes and ketenes, and they can be represented by resonance structures **1a**, **1b**, and **1c**. Electrophiles tend

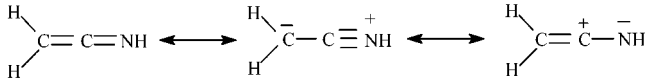

**1a** **1b** **1c**

to approach $C_\beta$[2a] or N[2b] of ketenimines, while nucleophiles readily attack $C_\alpha$ of ketenimines.[2] Ketenimines have attracted considerable interest as substrates for the synthesis of heterocycles, largely through processes involving cycloaddition reactions.[3] Kinetic studies of hydration of ketenimines in a wide range of pH values have been carried out by Hegarty et al.[2a,b] and Kresge et al.,[4a] showing that the hydration mechanism of ketenimines under acidic conditions is substituent-dependent.[4b]

The mechanism of amination of ketenes has been studied by a number of authors and has led to some controversy.[5,6] In early studies, theoretical[5a,b] and kinetic[5c−e] studies of amination of ketenes were interpreted as involving initial addition to the C═C bond of ketenes. Later, high-level ab initio calculations[6a,b] and kinetic studies[6b−f] overthrew the previous mechanism and suggested that the amination proceeds via amine addition across the C═O bond of ketenes. Meanwhile, some labile intermediates of amide enols from amination of ketenes were caught by IR[6b,d,e] and UV,[6f] and a stable amide enol[6g] from amination of a crowded diarylketene was even isolated.

In comparison with ketenes, a mechanistic study of amination of ketenimines is lacking but it is known that

(1) Staudinger, H.; Hauser, E. *Helv. Chim. Acta* **1921**, *4*, 887.

(2) (a) McCarthy, D. G.; Hegarty, A. F. *J. Chem. Soc., Perkin Trans. 2* **1980**, 579. (b) Hegarty, A. F.; Kelly, J. G.; Relihan, C. M. *J. Chem. Soc., Perkin Trans. 2* **1997**, 1175. (c) Krow, G. R. *Angew. Chem., Int. Ed. Engl.* **1971**, *10*, 435. (d) Barker, M. W.; McHenry, W. E. *The Chemistry of Ketenes, Allenes and Related Compounds*, Part 2; John Wiley & Son: New York, 1980; p 701. (e) Perst, H. *Methoden der Organischen Chemie* (Houben-Weyl), Stuttgart: New York, 1993; Vol. E15, Part 3, pp 2531−2710.

(3) (a) Barbaro, G.; Battaglia, A.; Giorgianni, P.; Giacomini, D. *Tetrahedron* **1993**, *49*, 4293. (b) Carisi, P.; Mazzanti, G.; Zani, P.; Barbaro, G.; Battaglia, A.; Giorgianni, P. *J. Chem. Soc., Perkin Trans. 1* **1987**, 2647. (c) Molina, P.; Alajarin, M.; Vidal, A.; Fenau-Dupont, J.; Declerq, J. P. *J. Org. Chem.* **1991**, *56*, 4008. (d) Dondoni, A. *Heterocycles* **1980**, *14*, 1547. (e) Alajarin, M.; Molina, P.; Vidal, A.; Tovar, F. *Tetrahedron* **1997**, *39*, 13449. (f) Schmittel, M.; Steffen, J.-P.; Angel, M. A. W.; Engels, B.; Lennartz, C.; Hanrath, M. *Angew. Chem., Int. Ed.* **1998**, *37*, 1562.

(4) (a) Chiang, Y.; Grant, A. S.; Guo, H.-X.; Kresge, A. J.; Paine, S. W. *J. Org. Chem.* **1997**, *62*, 5363. (b) McCarthy, D. G.; McCutcheon, P. O.; Sheehan, D. P. *J. Chem. Soc., Perkin Trans. 1* **1994**, 2899.

(5) (a) Lee, I.; Song, C. H.; Uhm, T. S. *J. Phys. Org. Chem.* **1988**, *1*, 83. (b) Lillford, P. J.; Satchell, D. P. N. *J. Chem. Soc. B* **1970**, 1016. (c) Lillford, P. J.; Satchell, D. P. N. *J. Chem. Soc. B* **1967**, 360. (d) Briody, J. M.; Satchell, D. P. N. *Tetrahedron* **1966**, *22*, 2649. (e) Lillford, P. J.; Satchell, D. P. N. *J. Chem. Soc. B* **1968**, 54.

(6) (a) Sung, K.; Tidwell, T. T. *J. Am. Chem. Soc.* **1998**, *120*, 3043. (b) Raspoet, G.; Nguyen, M. T.; Kelly, S.; Hegarty, A. F. *J. Org. Chem.* **1998**, *63*, 9669. (c) Allen, A. D.; Tidwell, T. T. *J. Org. Chem.* **1999**, *64*, 266. (d) Wagner, B. D.; Arnold, B. R.; Brown, G. W.; Lusztyk, J. *J. Am. Chem. Soc.* **1998**, *120*, 1827. (e) de Lucas, N. C.; Netto-Ferreira, J. C.; Andraos, J.; Lusztyk, J.; Wagner, B. D.; Scaiano, J. C. *Tetrahedron Lett.* **1997**, *38*, 5147. (f) de Lucas, N. C.; Netto-Ferreira, J. C.; Andraos, J.; Scaiano, J. C. *J. Org. Chem.* **2001**, *66*, 5016. (g) Frey, J.; Rappoport, Z. *J. Am. Chem. Soc.* **1996**, *118*, 3994.

10.1021/jo025523z CCC: $22.00 
Published on Web 05/07/2002

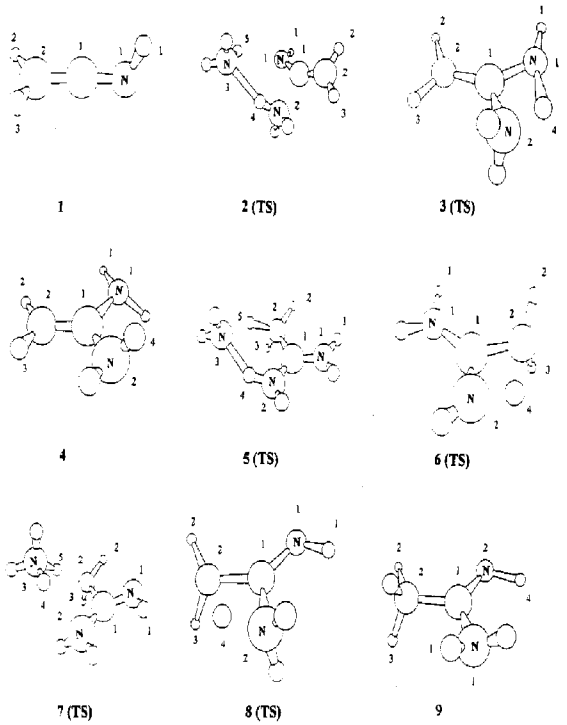


**Figure 1.** Optimized structures of **1**−**9** at the HF/6-31+G* level.

amination of ketenimines forms amidines.[2b,7] We wonder if the addition occurs across the C=C bond or the C=N bond of ketenimines? The addition across the C=C bond would cause the amination to be a concerted reaction, while the addition across the C=N bond would make the amination stepwise. If the addition occurs across the C=N bond, then vinylidenediamines would be intermediates. Can they be isolated or observed in solution? In this paper we try to solve the issue using low-temperature NMR spectra and by ab initio calculations in both the gas phase and solvent.

## Computational Details

All the calculations reported here were performed with the Gaussian98 program.[8] Geometry optimizations of ketenimine **1**, **2(TS)**, **3(TS)**, **4**, **5(TS)**, **6(TS)**, **7(TS)**, **8(TS)**, **9**, **13**, and ammonia were carried out at the HF/6-31+G* level in both gas phase and the solvent ($\epsilon$ = 35.9) without any symmetry restriction, except for **7(TS)** whose dihedral angles of H4−N2−C1−C2 and N3−H4−N2−C1 were fixed. Optimized structures and structural formulas of **1**−**9** are shown in Figure 1 and Scheme 1. The structural formula of **13** is shown in the Results and Discussion and it is a vinylidenediamine with a zwitterion structure. The Onsager self-consistent reaction field (SCRF) model[9] has been used to monitor systems in a solvent of dielectric constant of 35.9 which is close to that of acetonitrile.[9b] The model treats the solvent as a continuum of uniform dielectric constant $\epsilon$ (the reaction field) and the solute is placed into a fixed spherical cavity of radius $a_0$ within the solvent. The radius $a_0$ of the cavity for each solute was evaluated on the basis of its optimized structure in the gas phase. Geometry optimizations of *trans*-**11**, *cis*-**11**, **14(TS)**, and **15(TS)** were carried out at the B3LYP/6-31G* level in the gas phase, and their optimized structures are shown in Figure 3. After all the geometry optimizations were performed, analytically vibrational frequencies were calculated at the same level to determine the nature of the located stationary points. Thus, all the stationary points found were properly characterized by evaluation of the harmonic frequencies. Single-point energies of the optimized structures of **1**−**9** and ammonia were carried out by density functional theory (DFT) at the B3LYP/6-311+G(2d,p)//HF/6-31+G* level in gas phase and at the MP2/6-31+G* level in the solvent, and energies of all the stationary points were calculated at the same level with scaled zero-point vibrational energies included. A scaled factor of 0.8929 for zero-point vibrational energies is used according to the literature.[9b,10]

**Scheme 1**

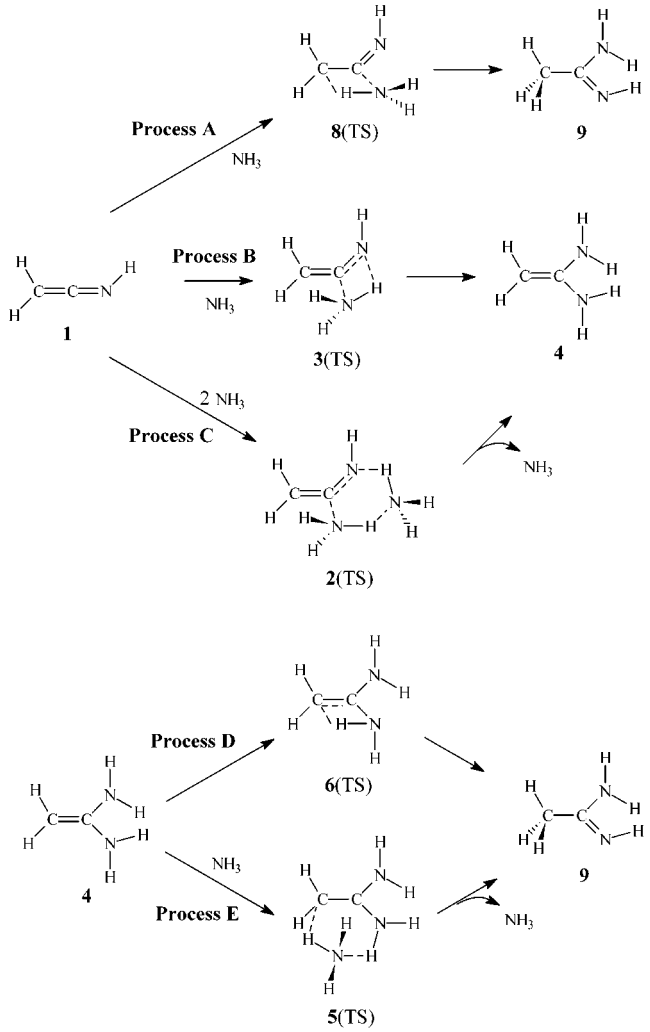


(7) (a) Li, Y.-Z.; Kirby, J. P.; George, M. W.; Poliakoff, M.; Schuster, G. B. *J. Am. Chem. Soc.* **1988**, *110*, 8092. (b) Motoyoshiya, J.; Teranishi, A.; Mikoshiba, R.; Yamamoto, I.; Gotoh, H. *J. Org. Chem.* **1980**, *45*, 5385. (c) Goerdeler, J.; Laqua, A.; Lindner, C. *Chem. Ber.* **1980**, *113*, 2509. (d) Stevens, C.; Freeman, R.; Noll, K. *J. Org. Chem.* **1965**, *30*, 3718.

(8) Frisch, M. J.; Trucks, G. W.; Schlegel, H. B.; Scuseria, G. E.; Robb, M. A.; Cheeseman, J. R.; Zakrzewski, V. G.; Montgomery, J. A., Jr.; Stratmann, R. E.; Burant, J. C.; Dapprich, S.; Millam, J. M.; Daniels, A. D.; Kudin, K. N.; Strain, M. C.; Farkas, O.; Tomasi, J.; Barone, V.; Cossi, M.; Cammi, R.; Mennucci, B.; Pomelli, C.; Adamo, C.; Clifford, S.; Ochterski, J.; Petersson, G. A.; Ayala, P. Y.; Cui, Q.; Morokuma, K.; Malick, D. K.; Rabuck, A. D.; Raghavachari, K.; Foresman, J. B.; Cioslowski, J.; Ortiz, J. V.; Stefanov, B. B.; Liu, G.; Liashenko, A.; Piskorz, P.; Komaromi, I.; Gomperts, R.; Martin, R. L.; Fox, D. J.; Keith, T.; AlLaham, M. A.; Peng, C. Y.; Nanayakkara, A.; Gonzalez, C.; Challacombe, M.; Gill, P. M. W.; Johnson, B.; Chen, W.; Wong, M. W.; Andres, J. L.; Gonzales, C.; Head-Gordon, M.; Replogle, E. S.; Pople, J. A. *Gaussian 98*, Revision A.9; Gaussian, Inc.: Pittsburgh, PA, 1998.

(9) (a) Wiberg, K. B.; Murcko, M. A. *J. Phys. Chem.* **1987**, *91*, 3616. (b) Foresman, J. B.; Frisch, A. *Exploring Chemistry with Electronic Structure Methods*, 2nd ed.; Gaussian, Inc.: Pittsburgh, PA, 1996.

(10) (a) Gong, L.; McAllister, M. A.; Tidwell, T. T. *J. Am. Chem. Soc.* **1991**, *113*, 6021. (b) McAllister, M. A.; Tidwell, T. T. *J. Org. Chem.* **1994**, *59*, 4506.

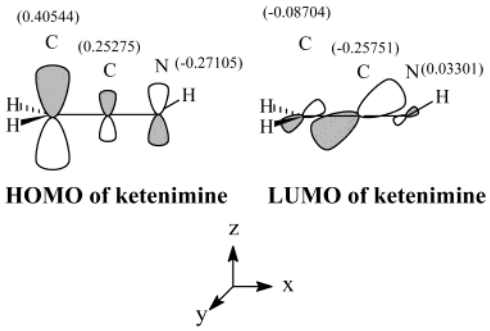


**Figure 2.** HOMO and LUMO of ketenimine **1** at the HF/6-31+G* level.

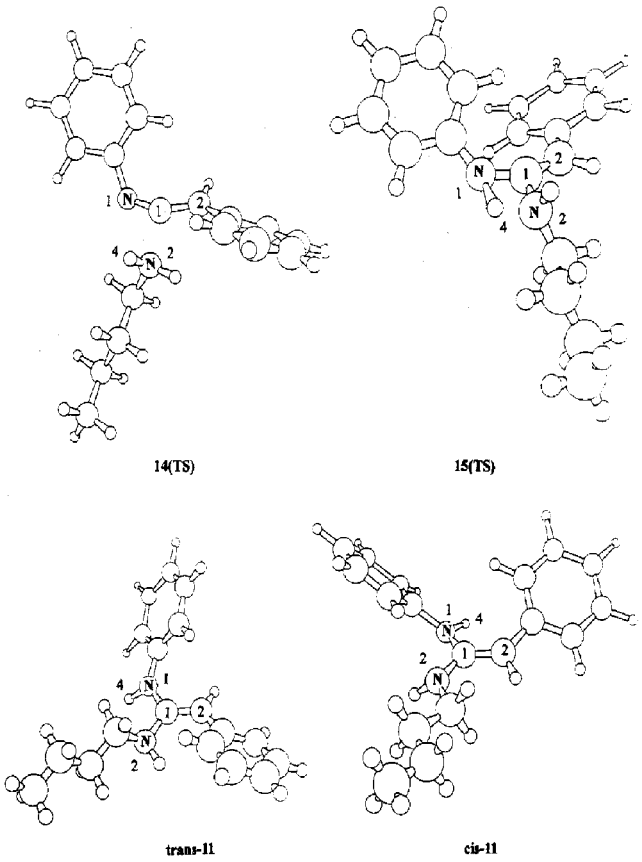


**Figure 3.** Optimized structures of **14(TS)**, **15(TS)**, *trans*-**11**, and *cis*-**11** at the B3LYP/6-31G* level.

All the occupied and virtual molecular orbitals of ketenimine **1** were calculated by full population analysis at the HF/6-31+G* level, and its HOMO and LUMO are shown in Figure 2.

Thermal energies and entropies of stationary points were calculated at HF/6-31+G* in both the gas phase and the solvent, and $\Delta H^{\ddagger}$(298 K), $\Delta S^{\ddagger}$(298 K), $\Delta G^{\ddagger}$(298 K), $\Delta H$(298 K), $\Delta S$(298 K), and $\Delta G$(298 K) were calculated at the B3LYP/6-311+G(2d,p)//HF/6-31+G* level in the gas phase and at the MP2/6-31+G*//HF/6-31+G* level in the solvent, as described by Jorgensen et al.[11]

NMR shielding constants of *trans*-**11**, *cis*-**11**, and tetramethylsilane were calculated at the HF/6-31G*//B3LYP//6-31G* level, and computed data are in reasonable agreement with experimental data.[9b] The chemical shift of each of the protons was computed relative to that of tetramethylsilane.

(11) Jorgensen, W. L.; Lim, D.; Blake, J. F. *J. Am. Chem. Soc.* **1993**, *115*, 2936.

**Table 1. Calculated Activation Enthalpies (kcal/mol), Activation Entropies (cal/mol K), Activation Free Energies (kcal/mol), Enthalpies (kcal/mol), Entropies (cal/mol K), and Free Energies (kcal/mol) for Amination of Ketenimine in the Gas Phase ($\epsilon = 1$) at the B3LYP/6-311+G(2d,p)//HF/6-31+G* Level and in Solvent ($\epsilon = 35.9$) at the MP2/6-31+G*//HF/6-31+G* Level (Onsager Model)**

| | $\Delta H^{\ddagger}_{298}$ | $\Delta S^{\ddagger}_{298}$ | $\Delta G^{\ddagger}_{298}$ | $\Delta H_{298}$ | $\Delta S_{298}$ | $\Delta G_{298}$ |
|---|---|---|---|---|---|---|
| Process A (C=C Addition) **1** + $NH_3$ → **8(TS)** → **9** | | | | | | |
| gas phase ($\epsilon = 1$) | 49.01 | −38.65 | 60.53 | −22.60 | −36.36 | −11.76 |
| solvent ($\epsilon = 35.9$) | 42.77 | −40.84 | 54.94 | −32.03 | −38.50 | −20.55 |
| Process B (C=N Addition) **1** + $NH_3$ → **3(TS)** → **4** | | | | | | |
| gas phase ($\epsilon = 1$) | 32.78 | −38.61 | 44.29 | −12.84 | −38.09 | −1.48 |
| solvent ($\epsilon = 35.9$) | 28.87 | −40.58 | 40.96 | −17.70 | −40.15 | −5.73 |
| Process C (C=N Addition) **1** + $2NH_3$ → **2(TS)** → **4** + $NH_3$ | | | | | | |
| gas phase ($\epsilon = 1$) | 21.77 | −64.38 | 40.97 | −12.84 | −38.09 | −1.48 |
| solvent ($\epsilon = 35.9$) | 16.61 | −67.54 | 36.75 | −17.70 | −40.15 | −5.73 |
| Process D (Uncatalyzed) **4** → **6(TS)** → **9** | | | | | | |
| gas phase ($\epsilon = 1$) | 45.76 | 0.72 | 45.55 | −9.76 | 1.73 | −10.27 |
| solvent ($\epsilon = 35.9$) | 46.55 | 2.54 | 45.79 | −14.33 | 1.65 | −14.82 |
| Process E ($NH_3$ Catalyzed) **4** + $NH_3$ → **5(TS)** → **9** + $NH_3$ | | | | | | |
| gas phase ($\epsilon = 1$) | 27.96 | −34.98 | 38.39 | −9.76 | 1.73 | −10.27 |
| solvent ($\epsilon = 35.9$) | 26.45 | −35.93 | 37.16 | −14.33 | 1.65 | −14.82 |

## Results and Discussion

**Ab Initio Studies of Amination of Ketenimine with $NH_3$.** All the optimized structures of stationary points along possible paths for amination of ketenimine with ammonia are shown in Figure 1 and Scheme 1. The structure of **7(TS)**, a transition state for two $NH_3$ additions across the C=C bond of ketenimine, cannot be optimized as a stationary point unless its dihedral angles of H4−N2−C1−C2 and N3−H4−N2−C1 are fixed at 42.2° and 14.6°, respectively. It turns out that the amination reaction does not follow this route.

The occupied and virtual molecular orbitals of ketenimine **1** were computed at the HF/6-31+G* level. As shown in Figure 2, its HOMO has a coefficient of 0.40544 for the $2P_z$ orbital of $C_\beta$, 0.25275 for the $2P_z$ orbital of $C_\alpha$, and −0.27105 for the $2P_z$ orbital of N. Its LUMO related to $\pi^*$ orbitals has a coefficient of −0.08704 for the $3P_y$ orbital of $C_\beta$, −0.25751 for the $3P_y$ orbital of $C_\alpha$, and 0.03301 for the $3P_y$ orbital of N. The HOMO of **1** is perpendicular to its molecular plane with the biggest coefficient on $C_\beta$, while the LUMO is in its molecular plane with the largest coefficient on $C_\alpha$. Therefore, attack on the $C_\alpha$ of ketenimine by a nucleophile would most likely be in-plane. Based on optimized structures of **2(TS)**, **3(TS)**, **14(TS)**, and **15(TS)** (Figures 1 and 3), it is clear that the amination of ketenimines does involve in-plane attack of amine nucleophiles on $C_\alpha$ of ketenimines.

Calculated activation enthalpies, activation entropies, activation free energies, enthalpies, entropies, and free energies of processes A−E in both the gas phase ($\epsilon = 1$) and the solvent ($\epsilon = 35.9$) are shown in Table 1 and Scheme 1. The activation free energy of process B (one $NH_3$ addition across the C=N bond of ketenimine) is much smaller than that of process A (one $NH_3$ addition across the C=C bond of ketenimine) by 13.98 kcal/mol in the solvent, but activation entropies of the both processes are very similar. The activation free energy of process B (one $NH_3$ addition across the C=N bond of ketenimine) is larger than that of process C (two $NH_3$ addition across the C=N bond of ketenimine) by 4.21 kcal/mol in the solvent, and the activation entropy of the latter is much smaller than that of the former by 26.96

cal/mol K. Therefore, both processes B and C are kinetically more favorable than process A in the solvent by 13.98 and 18.19 kcal/mol, respectively, indicating that the amination of ketenimine proceeds via amine addition across the C═N bond rather than the C═C bond.

The activation free energy of process E (tautomerization with catalysis of one $NH_3$) is much smaller than that of process D (tautomerization without catalysis) by 8.63 kcal/mol in the solvent, and the activation entropy of the latter is much smaller than that of the former by 38.47 cal/mol K. The activation free energy of process B (one $NH_3$ addition across the C═N bond of ketenimine) is smaller than that of process D (tautomerization without catalysis) by 4.83 kcal/mol, but larger than that of process E (tautomerization with catalysis of one $NH_3$) by 3.8 kcal/mol. The activation free energy of process C (two $NH_3$ addition across the C═N bond of ketenimine) is smaller than those of process D (tautomerization without catalysis) and process E (tautomerization with catalysis of one $NH_3$) by 9.04 and 0.41 kcal/mol, respectively. If the amination occurs by process B followed by process D, the activation free energy for the reverse reaction of the first step (the process B) is 46.69 kcal/mol, which is 0.9 kcal/mol larger than that of the second step (the process D), indicating that reversibility of the first step would be less likely. If the amination occurs by process C followed by process E, the activation free energy for the reverse reaction of the first step (process C) is 42.48 kcal/mol, which is 5.32 kcal/mol larger than that of the second step (process E), indicating that reversibility of the first step would be unlikely.

**Low-Temperature NMR Studies of Amination of *N*-Phenylphenylketenimine 10 with *n*-BuNH$_2$.** The amination reaction of **10** with a 50× excess of *n*-butylamine in $CD_3CN$ was studied at −10 °C by continuous monitoring of the $^1$H NMR spectra of the reaction solution. Due to a higher temperature mixing at the very beginning of the amination reaction, 46% of **10** was converted quickly to the final product **12**, 27% of **10** was converted into the intermediate **11**, and 27% of **10** remained unreacted ((b) in Figure 4). With the temperature of the mixture kept at −10 °C inside the NMR spectrometer, the formation rate of **12** was very slow, but both the disappearance rate of **10** and the formation rate of **11** were fast. Forty-five minutes later, **10** was consumed completely ((d) in Figure 4) and the amount of **11** stopped increasing and started decreasing slowly. The formation rate of **12** becomes very slow at the expense of consuming **11**. Nineteen hours later, some of the intermediate still remained. After warming the solution to room temperature, the rest of the intermediate disappeared and was converted into **12** in half an hour. A singlet resonance absorption of benzyl phenyl ether at $\delta$ 5.0 ppm was used to monitor the amount of **10**, **11**, and **12** during the amination reaction. As shown in Figure 4, yield of **12** is excellent (>99%) with few byproducts. The reaction and monitoring by NMR at −10 °C was repeated more than 10 times, and the same results were found every time. It turns out that the amination reaction involves two steps and the reaction rate of the first step is much faster than that of the second step. The result rules out the possibility that *n*-butylamine adds directly across the C═C bond of **10**, because the reaction would directly produce **12** if it occurred by this route.

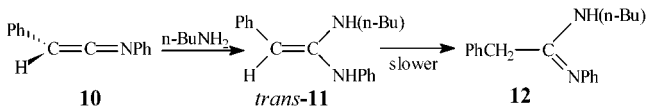


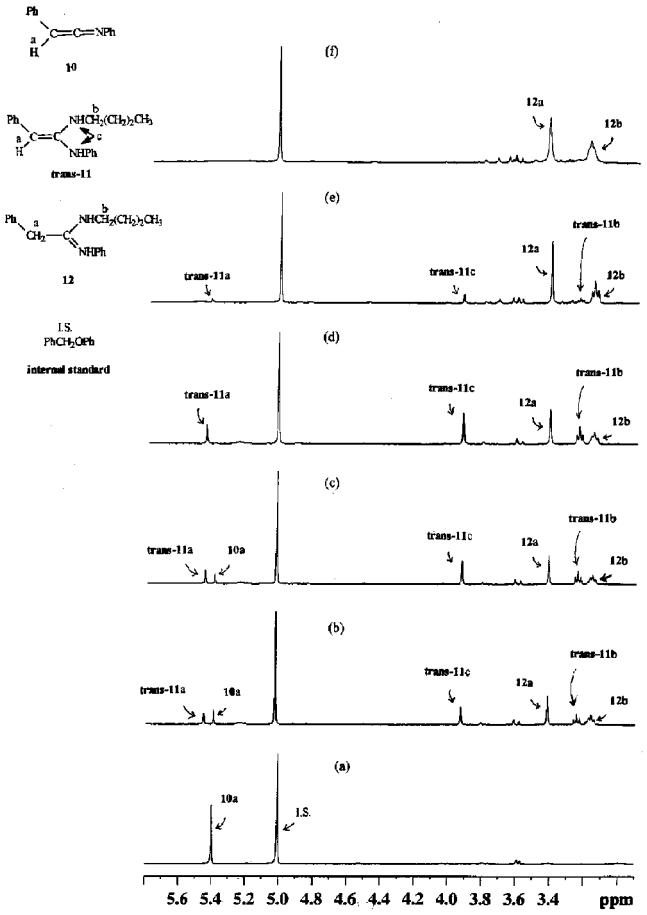


**Figure 4.** Part of $^1$H NMR ($CD_3CN$) spectra for the reaction of **10** (0.01 mmol) with *n*-butylamine (0.5 mmol) in the presence of an internal standard (benzyl phenyl ether, 0.033 mmol) at −10 °C (a) before adding *n*-butylamine, (b) at 10 min after mixing the solution, (c) at 14 min, (d) at 45 min, (e) at 19 h, and (f) at 30 min after increasing the temperature to 25 °C.

As shown in Figure 4, characteristic proton NMR resonance peaks during the amination reaction of **10** with *n*-butylamine are located at $\delta$ 5.384 (1H, s, C*H*═C═N) ppm for **10**, $\delta$ 3.420 (2H, s, C$H_2$−C(═NPh)N−Bu) and 3.163 (2H, t, NC$H_2$) ppm for amidine **12**, and $\delta$ 5.458 (1H, s, C*H*═C), 3.925 (2H, s, N*H*Ph and N*H*(*n*-Bu)), and 3.241 (2H, t, NC$H_2$) ppm for the intermediate **11**. Structure assignment of **10** and **12** is very clear, and they are ketenimine and amidine, respectively. However, the structure assignment of **11** is more subtle. There are two possible geometric isomers for **11**, but only one of them is present. The three characteristic NMR resonance peaks assigned to **11** maintain the same ratio of 1:2:2 when **11** grows or disappears, so it is very likely that the three resonance peaks come from the same intermediate. The characteristic peak at 3.241 ppm represents methylene protons close to the nitrogen of the *n*-butylamine group of **11**. The singlet peak at $\delta$ 5.458 ppm represents a vinyl hydrogen of **11**. When the reaction was monitored at −63 °C in DMF-$d_7$, the characteristic peak corresponding to the one at 3.925 ppm in $CD_3CN$ became broad while other characteristic peaks remain sharp. It is known that

protons on nitrogens of alkyl and arylamines have sharp singlet NMR resonance peaks due to fast exchange rate for the protons.[12] Therefore, the characteristic peak at 3.925 ppm is assigned as the NH absorption peak of **11**. It is unlikely that the intermediate is zwitterion **13**,

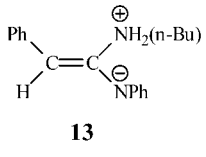


**13**

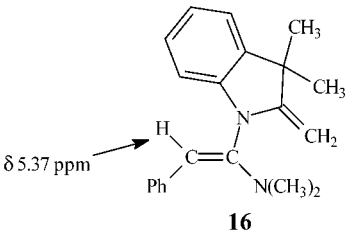


**16**

because protons on quaternary ammonium nitrogen have large downfield chemical shifts and exchange very slowly, causing very broad peaks.[12] In addition, the zwitterion **13** is not a stationary point on the potential energy surface at the HF/6-31+G* level. As for the proton on the nitrogen of amidine **12**, it also exchanges slowly with a broad peak[12] at 5.22 ppm but sometimes it is too broad to be found.

The intermediate **11** can be either the cis or trans isomer. NMR spectra of both isomers of **11** were studied by ab initio calculations at the HF/6-31G*//B3LYP/6-31G* level. The computed resonance absorption of the vinyl hydrogen of *cis*-**11** appears at $\delta$ 4.4 ppm, but that of *trans*-**11** appears at $\delta$ 5.2 ppm which is in reasonable agreement with experimental NMR resonance absorption of **11** at $\delta$ 5.458 ppm. The downfield shift for the vinyl hydrogen of *trans*-**11** is attributed to additional diamagnetic deshielding from the *N*-phenyl ring. In addition, the electronic environment for the vinyl hydrogen of **16** is similar to that of *trans*-**11**, and the reported experimental chemical shift for the vinyl hydrogen of **16** is $\delta$ 5.37 ppm,[13] which is very close to $\delta$ 5.458 ppm for the intermediate **11**. Therefore, the intermediate **11** observed is very likely to be *trans*-**11**. However, according to computational results at the B3LYP/6-31G*//B3LYP/6-31G* level, *trans*-**11** is less stable than *cis*-**11** by 1.05 kcal/mol. To figure out why the reaction gives the intermediate *trans*-**11** with higher energy, transition states **14(TS)** and **15(TS)** for both routes were located and optimized at the B3LYP/6-31G*//B3LYP/6-31G* level, assuming that the amination reaction involves one *n*-butylamine addition to **10**. The transition state **14(TS)** going to *trans*-**11** is more stable than the transition state **15(TS)** going to *cis*-**11** by 6.46 kcal/mol. It turns out that the first step of the amination reaction is kinetic control, instead of thermodynamic control.

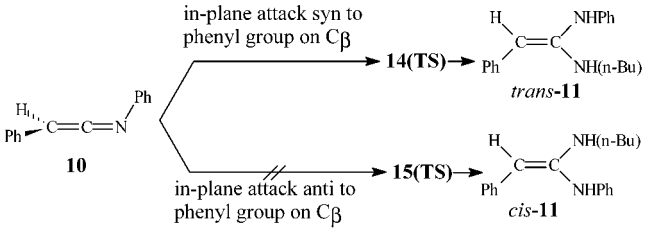


According to the computational results, a nucleophile does an in-plane attack on $C_\alpha$ of ketenimine. There are two sides of **10** for *n*-butylamine to do in-plane attack. One is an attack syn to the phenyl group on $C_\beta$ and the attack goes through **14(TS)** to produce *trans*-**11**. The reaction route may suffer a nonbonding interaction between the phenyl group and incoming *n*-butylamine. The other is an attack anti to the phenyl group on $C_\beta$, where there is no nonbonding interaction between the incoming *n*-butylamine and the phenyl group, and the attack goes through **15(TS)** to produce *cis*-**11**. However, apparently **14(TS)** does not really suffer a major nonbonding interaction involving the incoming *n*-butylamine, but in **15(TS)** the *N*-phenyl group is getting close to the phenyl group on $C_\beta$, causing a significant nonbonding interaction. As expected, according to optimized structures in Figure 3, **14(TS)** going to *trans*-**11** is an earlier transition state while **15(TS)** going to *cis*-**11** is a later transition state. Nonbonding interaction in **15(TS)** is much more significant than that in **14(TS)**, causing the amination reaction to proceed via **14(TS)** instead of **15(TS)**.

Some information about substituent effects on the amination reaction of ketenimine may be obtained by comparing optimized structures of **3(TS)**, **14(TS)**, and **15(TS)**. The C1−N2 bond distances of **3(TS)**, **14(TS)**, and **15(TS)** are 1.487, 1.920, and 1.508 Å, respectively, indicating that **14(TS)** is an earlier transition state than both **3(TS)** and **15(TS)**. The N1−C1−C2 bond angles of **3(TS)**, **14(TS)**, and **15(TS)** are 140.6, 146.7, and 142.7°, respectively, and these bond angles are halfway between the N1−C1−C2 bond angle (175.7°) of ketenimine and the N1−C1−C2 bond angles (ca. 123°) of vinylidenediamine intermediates. On the basis of the N1−C1−C2 bond angles of the transition states, it implies that the sequence of the earlier transition state is **14(TS)** > **15(TS)** > **3(TS)**, which is the same as the one predicted by means of their C1−N2 bond distances. The Ph−N1−C1−C2 dihedral angles of **14(TS)** and **15(TS)** and corresponding H1−N1−C1−C2 dihedral angle of **3(TS)** are 48.3, 32.4, and 0.0°, respectively, which give the same trend regarding the sequence of the earlier transition state. According to the N1−C1−C2 bond angles and the Ph−N1−C1−C2 dihedral angles of **14(TS)** and **15(TS)**, there is more significant bending of the C=C=N moiety and more significant rotation around the C1−N1 bond in **15(TS)** than in **14(TS)**, and indeed this is what causes the Ph−Ph interaction in **15(TS)**. In addition, due to the steric effect, bulky substituents on N1 and C2 of ketenimine may shift the transition state of amination of ketenimine to an earlier one in order to reduce destabilizing nonbonding interactions among the bulky substituents and the incoming amine.

Many reactions involving the second step as a rate-determining step have their first steps reversible, such as specific-acid-catalyzed reactions.[14] Since the second step of the amination reaction of **10** with *n*-butylamine is much slower than the first step, we wonder if the first step of the reaction is reversible? In other words, if the barrier of reverse reaction of the first step is low enough compared with the barrier of the second step, then the first step would be reversible. For the reaction of **10** with *n*-butylamine, only *trans*-**11** was found and no characteristic proton NMR resonance absorption for both **17** and

(12) Pavia, D. L.; Lampman, G. M.; Kriz, G. S. *Introduction to Spectroscopy*, 2nd ed.; Saunders College Publishing: New York, 1996.
(13) Fuks, R.; Viehe, H. G. *Chem. Ber.* **1970**, *103*, 573.
(14) Connors, K. A. *Chemical Kinetics*; VCH publishers, New York, 1990.

**18** could be found during the amination reaction. Even

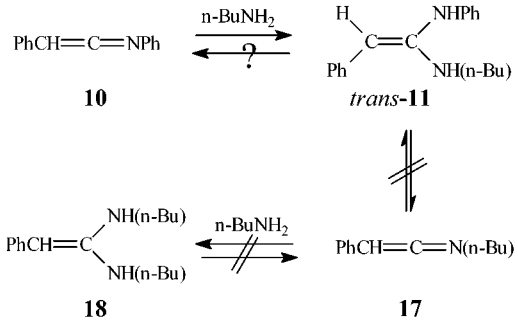


though NHPh and NH(*n*-Bu) look alike and NHPh is a better leaving group than NH(*n*-Bu), the above experiment cannot prove reversibility of the amination reaction. Further experiment involving the $H_2N^{15}Ph$ nucleophile may solve the problem.

## Conclusion

The HOMO of ketenimine is perpendicular to its molecular plane with the largest coefficient on $C_\beta$, while the LUMO is in its molecular plane with the largest coefficient on $C_\alpha$. An amine nucleophile reacts by an in-plane attack on $C_\alpha$ of ketenimine. The amination of ketenimine proceeds via amine addition across the C═N bond rather than the C═C bond, followed by tautomerization to form the amidine product, so it involves an intermediate of vinylidenediamine which is directly observed by low-temperature proton NMR spectra. The amination reaction of **10** with a 50× excess of *n*-butylamine in $CD_3CN$ produces amidine **12** via the less stable intermediate *trans*-**11**, and the first step is much faster than the second step. The first step is a kinetic-control reaction, which proceeds through the more stable transition state **14(TS)** rather than the less stable transition state **15(TS)** to the less stable intermediate *trans*-**11** rather than the more stable intermediate *cis*-**11**. In other words, in the reaction of **10** with *n*-$BuNH_2$, attack of *n*-$BuNH_2$ syn to the phenyl group on C$\beta$ of **10** is preferred, even though this produces a less stable product (*trans*-**11**); attack of *n*-$BuNH_2$ anti to the phenyl group on C$\beta$ of **10** is lacking and results in serious nonbonding interactions between the two phenyls of the ketenimine, as they are pushed together in this transition state.

## Experimental Section

**General.** Unless otherwise stated, reagents were obtained from commercial suppliers and used as received. NMR spectra were obtained using NMR spectrometers. Ketenimine **10**[2a,15a] and amidine **12**[15b] were prepared according to the literature method.[2a]

**NMR Study of Amination of Ketenimine 10.** A NMR tube filled with 0.5 mL of a $CD_3CN$ solution of ketenimine **10** (0.01 mmol) and benzyl phenyl ether (0.033 mmol, serving as an internal standard) was cooled by liquid nitrogen. Pure *n*-butylamine (50 $\mu$L, 0.5 mmol) was injected into the NMR tube through a rubber cap. The solution in the NMR tube was shaken in a cold bath and then put into the NMR spectrometer. Then the reaction was monitored by recording its proton NMR spectra at −10 °C until all of ketenimine **10** and most of the intermediate *trans*-**11** were consumed, and then the temperature was raised to 25 °C. A singlet resonance absorption of benzyl phenyl ether at $\delta$ 5.0 ppm was used as an internal standard to monitor the amount of **10**, *trans*-**11**, and **12** during the amination reaction.

**Acknowledgment.** Financial support by the National Science Council of Taiwan, Republic of China (NSC 89-2113-M-006-020), is gratefully acknowledged. We thank the National Center For High-performance Computing of Taiwan for computer time.

**Supporting Information Available:** The geometric data (Table S1, S2, and S3), total energies (including scaled ZPE) and the Cartesian or Z-matrix coordinates of the reactants, intermediates, transition states, and products discussed in this paper. This material is available free of charge via the Internet at http://pubs.acs.org.

JO025523Z

(15) (a) Ketenimine **10**: $^1$H NMR ($CD_3CN$) $\delta$ 5.383 (1H, s, CH), 7.046−7.411 (10H, m, PhH) ppm; $^{13}$C NMR ($CD_3CN$) $\delta$ 44.66, 119.85, 124.41, 127.56, 128.87, 129.12, 129.45, 134.39, 137.57, 169.26 ppm; IR (hexane) $\nu_{max}$ 2019 cm$^{-1}$ (C═C═N); HRMS(EI) for $C_{14}H_{11}N$ *m/z* calcd 193.0891, found 193.0894. (b) Amidine **12**: $^1$H NMR ($CD_3CN$) $\delta$ 0.862 (3H, t, $CH_3$), 1.240 (2H, m, $CH_2$), 1.426 (2H, m, $CH_2$), 3.163 (2H, t, $NCH_2$), 3.420 (2H, s, $CH_2$), 6.638−7.316 (10H, m, PhH) ppm. Anal. Calcd for $C_{18}H_{21}N$: C 81.47, H 10.55, N 7.98. Found: C 81.44, H 10.48, N 8.01.